Journal of Advanced Research 24 (2020) 391–396

Contents lists available at ScienceDirect

Journal of Advanced Research

journal homepage: www.elsevier.com/locate/jare

Spin Seebeck effect in bipolar magnetic semiconductor: A case of magnetic MoS_2 nanotube

Guangqian Ding [a], Yonglan Hu [a], Dengfeng Li [a], Xiaotian Wang [b], Dan Qin [c]

[a] School of Science, Chongqing University of Posts and Telecommunications, Chongqing 400065, China
[b] School of Physical Science and Technology, Southwest University, Chongqing 400715, China
[c] Physics Department, Binzhou Medical University, 264003 Yantai, Shandong, China

GRAPHICAL ABSTRACT

Device model based on zigzag magnetic MoS_2 nanotube and the calculated spin-dependent currents through the device.

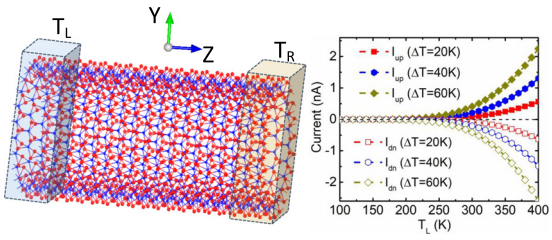

ARTICLE INFO

Article history:
Received 4 February 2020
Revised 21 April 2020
Accepted 4 May 2020
Available online 17 May 2020

Keywords:
MoS_2 nanotube
Spin caloritronic
First-principles
Bipolar magnetic semiconductor

ABSTRACT

Bipolar magnetic semiconductors (BMSs) are a new member of spintornic materials. In BMSs, one can obtain 100% spin-polarized currents by means of the gate voltage. However, most of previous studies focused on their applications in spintronics instead of spin caloritronics. Herein, we show that BMS is an intrinsic model for spin Seebeck effect (SSE). Without any gate voltage and electric field, currents with opposite spin orientation are generated and flow in opposite directions with almost equal magnitude when simply applying a temperature bias. This is also due to the special electronic structure of BMS where the conduction and valence bands near the Fermi level belong to opposite spin orientation. Based on density function theory and non-equilibrium Green's function methods, we confirm the thermal-induced SSE in BMS using a case of magnetic MoS_2 nanotube. The magnitude of spin current in zigzag tube is almost four times higher than that in armchair tube. BMS is promising candidates for spin caloritronic applications.

Introduction

The observation of spin Seebeck effect (SSE) is a remarkable achievement of spin caloritronics, a subject which combines spintronics and calorifics in a material [1,2]. To achieve SSE, the spin-polarized currents should be generated and flow in opposite directions in the device by a temperature gradient instead of any other external field, this requires apposite conduction and valence spin channels approaching to the Fermi level (E_F) [3,4]. The Joule heating is inhibited in the device under a pure spin currents, providing alternative strategy for low-power-consumption technology. Notably SSE has been discovered in such materials as silicene nanoribbon [5], graphyne nanoribbon [6] and boron-nitrogen nanotube [7]. However, the spin channel seems

Peer review under responsibility of Cairo University.

E-mail addresses: dinggq@cqupt.edu.cn (G. Ding), xiaotianwang@swu.edu.cn (X. Wang), qindan_ok@163.com (D. Qin)

https://doi.org/10.1016/j.jare.2020.05.006
2090-1232/

uncontrollable since it depends on the configuration and dimension of these nanostructures. Thus, a temperature induced SSE with pure and stable spin-polarized currents is still challenging.

In this work, we show that BMS is an intrinsic and stable model for SSE, which completely meets the requirements of SSE. BMS was proposed by Yang *et al.* [8] to achieve 100% spin-polarized current utilizing a gate voltage. The schematic density of states of BMS is given in Fig. 1c. From this figure, one can see that BMS are actually belonging to spin-polarized semiconductors (SPSs). However, different from common SPSs, the conduction bands (CBs) and valence bands (VBs) in BMSs near the E_F are belonging to carriers with opposite spin orientation. According to Yang *et al.* [8], adjusting the position of the E_F using a gate voltage realizes reversible half-metallicity in BMS. This can be applied to a spintronic device with bipolar field-effect spin-filter. For practical application, the band gap (BG) of BMS should have small value to ensure the feasibility of manipulating the spin-polarized currents. From another point of view, the electronic structure of BMS rightly meets the generation of SSE, which also provides a alternative applications in spin caloritronics. While it is worthwhile to note that not all BMS materials are ideal candidates for perfect SSE since the two spin channels may not completely symmetrical. In some cases, this could be optimized by tuning the position of the Fermi level using a gate voltage.

To clearly show how SSE occurs in BMS, we study the thermal spin transport (TST) characters of magnetic MoS_2 nanotube (NT) using first-principles density function theory (DFT) and non-equilibrium Green's function (NEGF) methods. Controlling synthesis of MoS_2 NT is already a proven technique [9], and various field-effect transistors based on MoS_2 NT show good performance [10,11]. DFT calculations reveal the semiconducting feature of MoS_2 NT [12]. However, to control the electrical, optical, and even magnetic properties for more potential applications, doping the semiconducting MoS_2 NT with minute amounts of foreign atoms is desirable, and this has been demonstrated by Tenne *et al.* [13]. Based on Kim *et al.* [14], substitution on Mo site with *3d* transition metals (V, Mn, Fe, Co and Cr) can induce notable magnetic moments, which transforms the semiconducting MoS_2 NT to one-dimensional magnetic semiconductor. Herein, our calculations are based on magnetic MoS_2 nanotube with Cr as the impurity.

Device model and computational methods

In term of the description of carbon NTs [15,16], the MoS_2 NT can also be distinguished according to the factor n and m, these are $n = m$ "armchair" nanotube and $n \neq 0$, $m = 0$ "zigzag" nanotube. Fig. 1a and Fig. 1b are the device models based on magnetic MoS_2 NT with zigzag and armchair configurations, respectively, and in the right panels of Fig. 2a and 2b are the side views. Seifert *et al* [12]. have studied the structure and electronic properties of MoS_2 NTs with the diameter ranging from 8 to 26 Å, corresponding to the indices $(n, n)/(n, 0)$ from (6, 6)/(10, 0) to (14, 14)/(22, 0), respectively. The experimental tube usually has larger diameter ~ 25 nm, and the largest diameters are in consistent with the smallest experimentally discovered tubes based on Seifert *et al* [12]. Here, our calculations are based on (14, 14) zigzag and (22, 0) armchair MoS_2 NTs. To induce magnetism, one Mo in unit tube is substituted by Cr.

We carry out the structural relaxation and electronic band structure calculations via DFT method within the generalized gradient approximation (GGA) Perdew-Burke-Eenzerhof (PBE) correlation functional implemented in VASP [17,18]. We use projector augment wave potential and a plane wave energy cutoff of 450 eV. A Monkhorst-Pack k-points of $1 \times 1 \times 21$ is used. The lattice and atom's positions are totally relaxed until the maximum force becomes less than 0.01 eV/Å. We set a precision of 10^{-6} eV for the criterion of the self-consistent total energy. A vacuum spacing of 15 Å is imposed to avoid the interaction between neighbor-

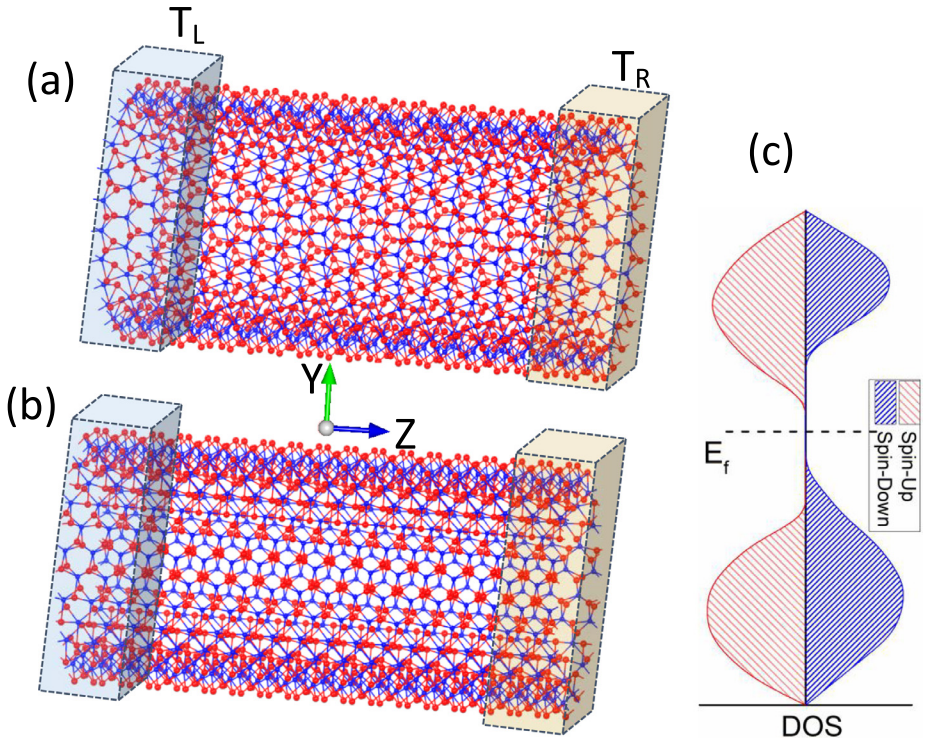

Fig. 1. Device models based on zigzag (a) and armchair (b) magnetic MoS_2 NT, T_L and T_R denote the temperatures of source and drain, respectively. (c) shows the schematic density of states of BMS.

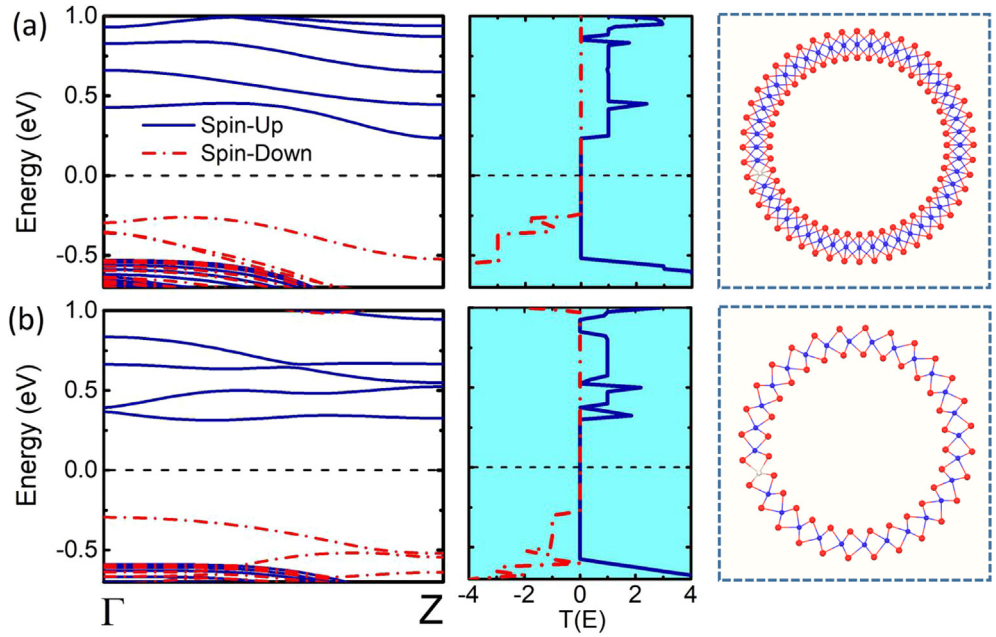

Fig. 2. The left, middle, and right panels respectively represent the calculated band structure, transmission spectrum, and structure in side view of the zigzag (a) and armchair (b) NTs.

ing NTs. Considering the energy gap underestimation of GGA function, we also adopt the modified Becke-Johnson (MBJ) [19] function in this work to ensure that we can achieve more accurate band structures. The TST calculations are then carried out via NEGF/DFT methods within Atomistix ToolKit (ATK) code [20–22]. We set the cutoff energy and the Monkhorst-Pack *k*-points as 150 Ry and $1 \times 1 \times 100$, respectively. The infinitesimal energy for the iteration of transmission spectrum is set as 10^{-6} eV, and we increase the sampling points to 201 in order to obtain the accurate transmission curves. Additionally, we consider a Double-Zeta-Polarized (DZP) basis set to obtain the accurate results. These computational details are common and reliable for the theoretical investigation of TST properties. According to the Landauer-Büttiker formula, the spin-dependent current is given by the following equation [23,24],

$$I^{\uparrow(\downarrow)} = \frac{e}{h}\int_{-\infty}^{\infty}\left\{T^{\uparrow(\downarrow)}(E)[f_L(E,T_L) - f_R(E,T_R)]\right\}dE \quad (1)$$

where $T_{L(R)}$ and $f_{L(R)}$ are the temperature and Fermi-Dirac distribution of left and right electrodes, respectively. $T^{\uparrow(\downarrow)}(E)$is the spin-dependent transmission function, which is determined by the retarded/advanced Green's functions of the central scattering region and also the coupling between the central scattering region and the left (right) electrode. Herein, we pay our attentions to the spin-dependent currents in the NT induced by temperature bias without any external field or gate voltage.

Results and discussion

Calculated band structures of (14, 14) zigzag and (22, 0) armchair MoS_2 NTs indicate that they are ideal BMS materials, as shown in the left panel of Fig. 2a and 2b, respectively. Based on the investigation of Yang *et al.* [8], MoS_2 NTs hold the advantages in spintronic applications due to its half-metallic behaviors are very robust and its opposite spin polarization can be obtained via the effect of electron/hole doping. Instead of focusing on their applications in spintronics, we here discuss the potential application in spin caloritronics. Both the zigzag NT and armchair NT features obvious indirect BGs around the E_F, and values of BGs are about 0.5 eV, while larger BG is found in armchair NT. Moreover, zigzag NT exhibits remarkable band dispersion as compared to armchair NT, which indicates the smaller effective mass and higher mobility of carriers in zigzag NT. These band features are important because of their non-negligible influence on the magnitude of current through the device. It is important in BMS that CBs and VBs, above and below the E_F, belong to opposite spin orientation. For magnetic MoS_2 NTs, there are spin-up conduction and spin-down valence bands approaching to the E_F, and these spin-up CBs and spin-down VBs occupy a remarkable energy span, which means that two opposite spin transport channels could be generated in the device under an external field. This is beneficial to the emergence of notable SSE when a temperature bias is applied, i.e., the spin-up and spin-down currents arise and flow in opposite directions, as long as the two opposite spin channels are nearly symmetrical [5].

Calculated transmission spectrum of zigzag and armchair NTs devices without a gate voltage are shown in the middle panel of Fig. 2a and b. Consistent with the electronic band characteristics, transmission channels belonging to opposite spin orientation can be distinguished above and below the E_F. It is easy to obtain a spintronic device by adjusting the E_F up or down through a gate voltage, which produces 100% spin polarization. In addition, the spin-dependent currents primarily depend on the net transmission around the E_F according to the formula of spin currents described in Eq. (1). Hence, when a temperature bias is applied to the device, it is desirable to generate spin-dependent currents flowing in opposite directions, and thus occur the SSE [5,25]. To confirm these analysis, we have to discuss the TST through the devices.

When calculating the TST properties, the spin-dependent current is driven by simply a temperature bias (ΔT) without any external voltage. The temperature bias is defined as $\Delta T = T_L - T_R$, where T_L and T_R denote the temperature of the source (left-electrode) and drain (right-electrode), respectively. During the calculation, the drain is set as high temperature. Because the

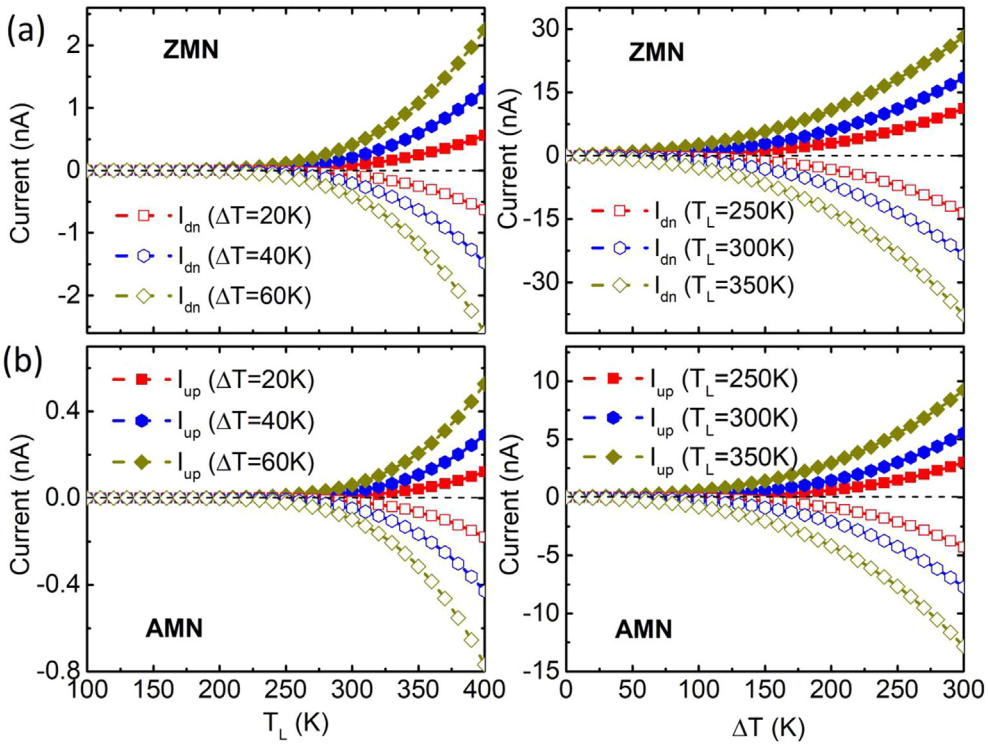

Fig. 3. Calculated spin-dependent currents (I_{up} and I_{dn}) of (a) zigzag magnetic NT (ZMN) and (b) armchair magnetic NT (AMN), the left and right panels denote the currents versus source temperature (T_L) and temperature bias (ΔT), respectively.

source and drain belong to same material and have the same electronic structure, carrier concentration between source and drain depends on the Fermi-Dirac distribution ($f_L(E, T_L)$-$f_R(E,T_R)$) [5,7], which is primarily determined by the temperature bias. When the temperature bais is applied, electrons and holes with energy higher and lower than the E_F will simultaneously transport from the drain to source, giving rise to electron current I_e and hole current I_h flowing in the opposite directions. For BMS, the spin-polarized transport channels leads to the spin-dependent currents, i.e., the spin-up $I_{e\uparrow}$ and spin-down $I_{h\downarrow}$. If the spin channels are highly symmetrical, the charge current is inhibited since $I_{e\uparrow}$ and $I_{h\downarrow}$ are counteracted, which called perfect SSE [5,7].

Calculated spin-dependent currents versus the source temperature (T_L) and temperature bias (ΔT) are shown in the left and right panels of Fig. 3, respectively. Results in Fig. 3a and 3b belong to the devices based on zigzag and armchair NTs, respectively. Since $f_L(E, T_L)$-$f_R(E,T_R)$ is an odd function, the sign of current depends on the slop of the transmission coefficient T(E) near the E_F according to Eq (1). We expect opposite signs for spin-up current (I_{up}) and spin-down one (I_{dn}) as the spin-up and spin-down transmission channels are located above and below the E_F, respectively. As shown in Fig. 3, the $I_{up} > 0$ while I_{dn} less than 0. It is clearly found that I_{up} and I_{dn} are generated via the ΔT without any external voltage, which arises individually from the spin-splitting electrons and holes flowing from the drain to source. Remarkably, the amplitudes of I_{up} and I_{dn} are almost the same in the whole temperature region, which indicates that an ideal SSE is achieved by BMS characteristic. As the increase of ΔT, the spin currents increase. The threshold temperatures (T_{th}) arise from the BGs, and the higher T_{th} of armchair NT is ascribed to its larger BG, as found in Fig. 3a and b. Moreover, it is compelling that currents in zigzag device is higher than that in armchair one, primarily due to the smaller BG and higher carrier mobility of zigzag NT as discussed before. In general, an ideal SSE, characterized by the nearly same amplitudes and threshold temperature in I_{up} and I_{dn}, is achieved in BMS using the case of magnetic MoS_2 NTs.

To illuminate the generation of SSE, we also perform the calculations of the total charge current (I_c) and spin current (I_s) versus ΔT, as plotted in Fig. 4a. One can notice that the charge current is suppressed while the spin current increases with the increase of ΔT, which indicates that the spin current dominates the thermal-induced transport in the device. The suppressed charge current contributes to reduced Joule heating, hence, the SSE devices can be applied to waste heat recovery and low-power-consumption technology. Calculated current spectra J(E) shown in Fig. 4b also points to the emergence of SSE. The magnitude of current is determined by the area covered under the curve associated with axis J(E) = 0. Obviously, two areas of current spectra with opposite spin channels are nearly symmetrical about the E_F, also suggesting the generation of SSE. However, it is worthwhile to note that the SSE achieved in magnetic MoS_2 NT is not completely perfect since the a little higher spin-down current leads to the incompletely inhibited charge current as found in Fig. 4a. Even so, it is desirable to explore other BMS materials as candidates for excellent SSE. In addition, the SSE can be further optimized by adjusting the dopants or the position of the Fermi level. To date, many BMS materials have been reported, such as carbon nanotube [8], boron-nitrogen nanotube [7] and SiN-SiC nanofilm [26], etc. Wu *et al.* [7] also discovered the robust SSE in magnetic boron-nitrogen nanotube. Thus, our calculations and results can be easily extended to other BMS materials.

Conclusion

In summary, we have shown that BMS material is an ideal candidate for SSE, which is expected to generate nearly pure spin current simply via a temperature bias. Based on First-principles DFT combined with NEGF methods, the concept is clarified via a case of magnetic MoS_2 NT. No matter if it is the zigzag or armchair con-

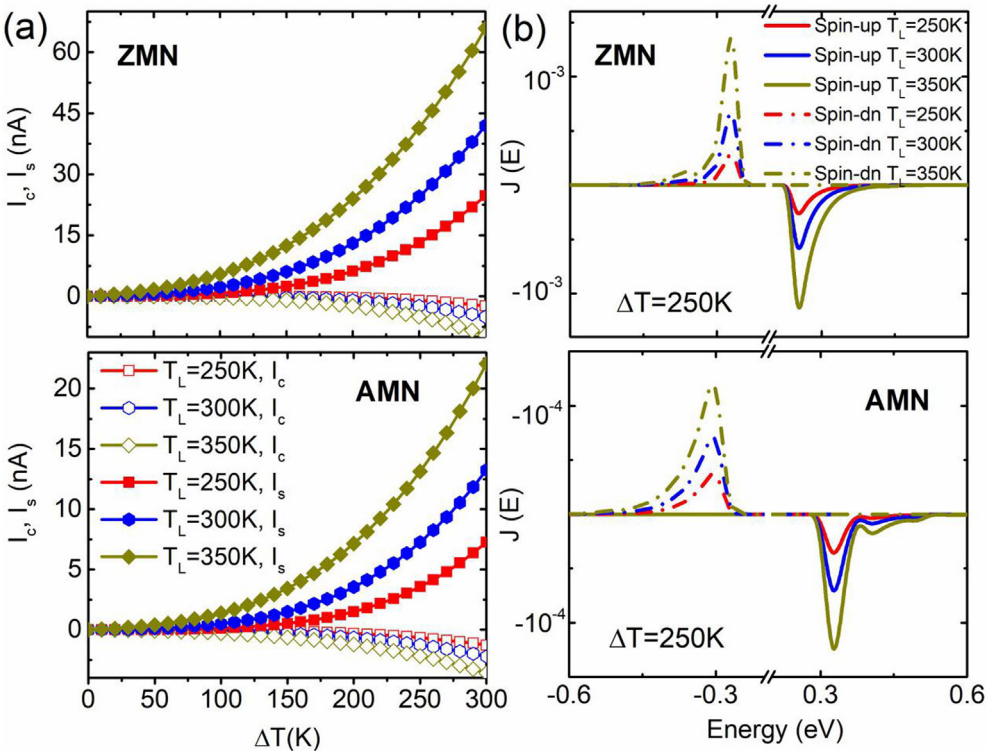

Fig. 4. (a) The calculated total spin current (I_s) and charge current (I_c) as a function of temperature bias (ΔT) for zigzag magnetic NT (ZMN) and armchair magnetic NT (AMN). (b) The spin-dependent current spectra at fixed ΔT = 250 K with different T_L.

figuration of the NT, the SSE is remained. Zigzag tube shows better transport performance, as its spin current is four times higher than that in armchair tube, which leads to the higher total spin current in zigzag tube, i.e., ~65nA at T_L = 350 K/ΔT = 300 K. Our study reveals the certainly application of BMS materials in spin caloritronic devices. Thus, through electrical control or heat management, BMS based multifunctional devices exhibit great flexibility of applications in not only spintronics but also spin caloritronics.

Compliance with ethics requirements

This article does not contain any studies with human or animal subjects.

Declaration of Competing Interest

The authors declare that they have no known competing financial interests or personal relationships that could have appeared to influence the work reported in this paper.

Acknowledgments

This work is supported by National Natural Science Foundation of China (Grant No.11804040) and Fundamental Research Funds for the Central Universities (Grant CQUPT: A2017-119).

References

[1] Uchida K, Takahashi S, Harii K, Ieda J, Koshibae W, Ando K, et al. Observation of the spin Seebeck effect. Nature 2008;455(7214):778–81.
[2] Jaworski CM, Myers RC, Johnston-Halperin E, Heremans JP. Giant spin Seebeck effect in a non-magnetic material. Nature 2012;487(7406):210–3.
[3] Adachi H, Uchida K, Saitoh E, Maekawa S. Theory of the spin Seebeck effect. Rep Prog Phys 2013;76(3):036501.
[4] Bosu S, Sakuraba Y, Uchida K, Saito K, Ota T, Saitoh E, et al. Spin Seebeck effect in thin films of the Heusler compound Co_2MnSi. Phys Rev B 2011;83(22):224401.
[5] Fu HH, Wu DD, Zhang ZQ, Gu L. Spin-dependent Seebeck Effect, Thermal Colossal Magnetoresistance and Negative Differential Thermoelectric Resistance in Zigzag Silicene Nanoribbon Heterojunciton. Sci Rep 2015;5(1):10547.
[6] Wu DD, Liu QB, Fu HH, Wu R. How to realize a spin-dependent Seebeck diode effect in metallic zigzag gamma-graphyne nanoribbons?. Nanoscale 2017;9(46):18334–42.
[7] Wu DD, Fu HH, Liu QB, Du GF, Wu R. Magnetic nanotubes: A new material platform to realize a robust spin-Seebeck effect and a perfect thermal spin-filtering effect. Phys Rev B 2018;98(11):115422.
[8] Li X, Wu X, Li Z, Yang J, Hou JG. Bipolar magnetic semiconductors: a new class of spintronics materials. Nanoscale 2012;4(18):5680–5.
[9] Nath M, Govindaraj A, Rao CNR. Simple synthesis of MoS_2 and WS_2 nanotubes. Adv Mater 2001;13(4):283–6.
[10] Fathipour S, Remskar M, Varlec A, Ajoy A, Yan R, Vishwanath S, et al. Synthesized multiwall MoS_2 nanotube and nanoribbon field-effect transistors. Appl Phys Lett 2015;106(2):022114.
[11] Strojnik M, Kovic A, Mrzel A, Buh J, Strle J, Mihailovic D. MoS_2 nanotube field effect transistors. AIP Adv 2014;4(9):097114.
[12] Seifert G, Terrones H, Terrones M, Jungnickel G, Frauenheim T. Structure and Electronic Properties of MoS_2 Nanotubes. Phys Rev Lett 2000;85(1):146–9.
[13] Yadgarov L, Rosentsveig R, Leitus G, Albu-Yaron A, Moshkovich A, Perfilyev V, et al. Controlled doping of MS_2 (M=W, Mo) nanotubes and fullerene-like nanoparticles. Angew Chem Int Ed Engl 2012;51(5):1148–51.
[14] Li N, Lee G, Jeong YH, Kim KS. Tailoring Electronic and Magnetic Properties of MoS_2 Nanotubes. J. Phys. Chem. C. 2015;119(11):6405–13.
[15] Abdel-Ghani NT, El-Chaghaby GA, Helal FS. Individual and competitive adsorption of phenol and nickel onto multiwalled carbon nanotubes. J Adv Res 2015;6(3):405–15.
[16] Eivazzadeh-Keihan R, Maleki A, de la Guardia M, Bani MS, Chenab KK, Pashazadeh-Panahi P, et al. Carbon based nanomaterials for tissue engineering of bone: Building new bone on small black scaffolds: A review. J Adv Res 2019;18:185–201.
[17] Perdew JP, Burke K, Ernzerhof M. Generalized gradient approximation made simple. Phys Rev Lett 1996;77:3865–8.
[18] Kresse GF, Furthmüller J. Efficient iterative schemes for ab initio total-energy calculations using a plane-wave basis set. Phys Rev B 1996;54:11169.
[19] Lugovskoi AV, Katsnelson MI, Rudenko AN. Strong Electron-Phonon Coupling and its Influence on the Transport and Optical Properties of Hole-Doped Single-Layer InSe. Phys Rev Lett 2019;123(17):176401.
[20] Brandbyge M, Mozos JL, Ordejón P, Taylor J, Stokbro K. Density-functional method for nonequilibrium electron transport. Phys Rev B 2002; 65: 165401.

[21] Soler JM, Artacho E, Gale JD, García A, Unquera J, Ordejón P, Sánchez-Portal D. The SIESTA method for ab initio order-N materials simulation, J Phys Condens Matter 2002; 14: 2745-79.
[22] Taylor J, Guo H, Wang J. Ab initio modeling of quantum transport properties of molecular electronic devices. Phys Rev B 2001;63:245407.
[23] Büttiker M, Imry Y, Landauer R, Pinhas S. Generalized many-channel conductance formula with application to small rings. Phys Rev B 1985;31:6207–15.
[24] Imry Y, Landauer R. Conductance viewed as transmission. Rev Mod Phys 1999;71:S306–12.
[25] Ding G, Wei M, Surucu G, Liang Z, Wang X. Transition metal-doped janus monolayer SMoSe with excellent thermal spin filter and spin Seebeck effect. Appl Surf Sci 2019;491:750–6.
[26] Zhang J, Li X, Yang J. SiN-SiC nanofilm: A nano-functional ceramic with bipolar magnetic semiconducting character. Appl Phys Lett 2014;104:172403.